

# Decay rate and renormalized frequency shift of superradiant exciton in a cylindrical quantum wire

Yueh-Nan Chen\* and Der-San Chuu†

*Department of Electrophysics, National Chiao-Tung University, Hsinchu 30050, Taiwan*

(Dated: November 10, 2018)

The decay rate and renormalized frequency shift of superradiant exciton in a cylindrical quantum wire are studied. The transition behavior from 1D wire to 2D film is examined through the property of the radiative decay. Similar to the case in a quantum well, the decay rate of the higher mode exciton is larger than that of the lower mode one. Moreover, it is also found the decay rate and frequency shift do not show oscillatory dependence on wire radius because of the conservation of angular momentum.

PACS: 42.50.Fx, 32.70.Jz, 71.35.-y, 71.45.-d

Since Dicke[1] pointed out the concept of superradiance, the coherent effect for spontaneous radiation of various systems has attracted extensive interest both theoretically and experimentally [2, 3, 4, 5]. In bulk crystal, the excitons will couple with photons to form polaritons[6]-mixed modes in which energy oscillates back and forth between the exciton and the radiation field. What makes the excitons trapped in the bulk crystal is the conservation of crystal momentum. If one considers a thin film[7], the excitons can undergo radiative decay as a result of the broken crystal symmetry along the normal direction of the film plane. The decay rate of excitons in a thin film is enhanced by a factor of  $(\lambda/d)^2$  compared to a lone exciton in an empty lattice, where  $\lambda$  is the wave length of emitted photon and  $d$  is the lattice constant of the film.

Lots of investigations on the radiative linewidth of excitons in quantum wells have been performed. An abnormal increase of excitonic radiative lifetime with the decrease of well width below  $5nm$  for  $In_xGa_{1-x}As/InP$  quantum well was observed by Cebulla *et al.*[8]. Brandt *et al.*[9] measured the radiative lifetime of excitons in InAs quantum sheets and observed the increasing of radiative lifetime with the decreasing of well thickness. Hanamura[10] investigated theoretically the radiative decay rate of quantum dot and quantum well. The obtained results are in agreement with that of Lee and Liu's[7] prediction for thin films. Knoester[11] studied the radiative dynamics crossover from the small thickness, superradiant exciton regime to bulk crystal, polariton regime. The oscillating dependence of the radiative width of the exciton-like polaritons with the lowest energy on the crystal thickness was found. Recently, G. Björk *et al.*[12] examined the relationship between atomic and excitonic superradiance in thin and thick slab geometries. They demonstrated that superradiance can be treated by a unified formalism for atoms, Frenkel excitons, and Wannier excitons. In V. M. Agranovich *et al.*'s work[13], a detailed microscopic study of Frenkel exciton-polariton in

crystal slabs of arbitrary thickness was performed.

For lower dimensional systems, the decay rate of the exciton is enhanced by a factor of  $\lambda/d$  in a linear chain[14]. First observation of superradiant short lifetimes of excitons was performed by Ya. Aaviksoo *et al.*[15] on surface states of the anthracene crystal. A. L. Ivanov and H. Haug[16] predicted the existence of exciton crystal, which favors coherent emission in the form of superradiance, in quantum wires. Y. Manabe *et al.*[17] considered the superradiance of interacting Frenkel excitons in a linear chain. Recently, we have also shown the superradiant decay of the quantum wire exciton is greatly enhanced in a planar microcavity[18]. In this paper, the exciton is assumed to be confined in a hollow cylindrical quantum wire. The crossover of the superradiant decay rate of the exciton from a wire with small radius to the 2D limit is explicitly obtained. Moreover, the crossover of the coherent frequency shift from narrow wire to thin film is also investigated by using the method of renormalization[19, 20].

We consider a free exciton in a hollow cylindrical quantum wire lying on the  $z$  axis with simple cubic structure (Fig. 1). For the physical phenomenon we are interested in, we shall concentrate on the investigations of semiconductor quantum wires rather than existing carbon wires [21, 22] since the wavelength of the emitted photon is much larger than the diameter of the single-wall carbon tubes. The crossover behavior from 1D wire to 2D film may not be examined on carbon systems. However, we hope our model can serve as a first step toward the understanding of the exciton decay in carbon nanotubes.

If the difference between the inner radius( $\rho_<$ ) and outer radius( $\rho_>$ ) is much smaller than the effective Bohr radius of the exciton, i. e.  $\Delta L \ll a_{ex}$ , one may approximate that the exciton is confined on the cylindrical surface with radius  $\rho(\approx \rho_< \approx \rho_>)$ . This means the exciton is trapped in an infinite deep and narrow quantum wire. The radius  $\rho$  is about  $Nd/2\pi$ , where  $N$  is the number of lattice points in the circumference direction and  $d$  is the lattice spacing. If one further assumes the radius of the wire is much larger than the effective Bohr radius of the exciton, variations of the wire radius only cause few

\*Electronic address: ynchen.ep87g@nctu.edu.tw

†Electronic address: dschuu@cc.nctu.edu.tw

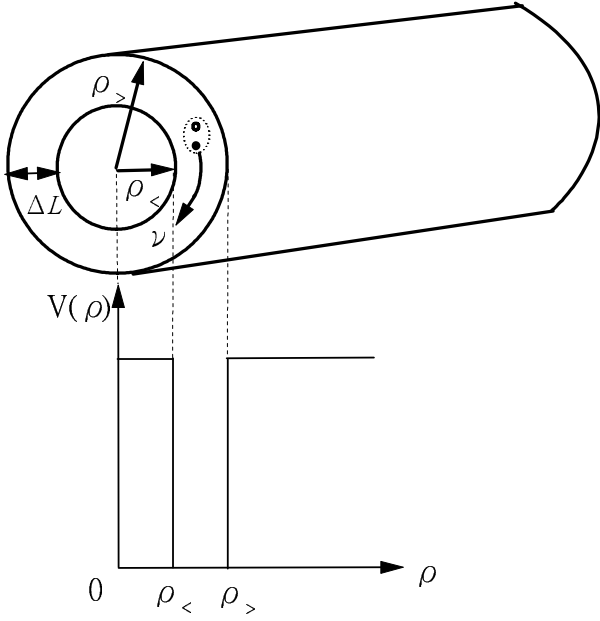


FIG. 1: Schematic view of the quantum wire structure and its defining potential profile.

changes on the Wannier exciton wavefunction. In this case, the main contributions to the *superradiant* decay rate and frequency shift still come from the bandgap energy and the number of the lattice points within a wavelength of the emitted photon[20]. Therefore, one can first consider the exciton as a particle with angular momentum  $\nu$  and longitudinal momentum  $k_z$ . After figuring out the decay rate and frequency shift of a Frenkel exciton, the corresponding ones of a Wannier Exciton can be obtained by replacing the single-atom dipole matrix element  $\chi$  with the effective dipole matrix element[7]. Thus, the Hamiltonian for the exciton is

$$H_{ex} = \sum_{\nu k_z} E_{\nu k_z} c_{\nu k_z}^\dagger c_{\nu k_z}, \quad (1)$$

where  $c_{\nu k_z}^\dagger$  and  $c_{\nu k_z}$  are the creation and destruction operators of the exciton, respectively. The Hamiltonian of free photon is

$$H_{ph} = \sum_{q'\nu'k'_z} \hbar c (q'^2 + k_z'^2)^{1/2} b_{q'\nu'k'_z}^\dagger b_{q'\nu'k'_z}, \quad (2)$$

where  $b_{q'\nu'k'_z}^\dagger$  and  $b_{q'\nu'k'_z}$  are, respectively, the creation and destruction operators of the photon. The wave vector  $\mathbf{k}'$  of the photon is separated into two parts:  $k'_z$  is the parallel component of  $\mathbf{k}'$  on the  $z$  direction such that  $k'^2 = q'^2 + k_z'^2$ .

The interaction between the exciton and the photon can be expressed as

$$H' = \sum_i \sum_{q'\nu'k'_z} \frac{e}{mc} \sqrt{\frac{2\pi\hbar c}{(q'^2 + k_z'^2)^{1/2}v}} (\boldsymbol{\epsilon}_{q'\nu'k'_z} \cdot \mathbf{p}_i) \times [b_{q'\nu'k'_z}^\dagger H_{\nu'}^{(1)}(q'\rho) \exp(i\nu'\varphi_i + ik'_z l_i) + \text{h.c.}], \quad (3)$$

where  $m$  is the electron mass,  $(\rho_i, \varphi_i, l_i)$  is the position of the electron  $i$  in the cylindrical wire,  $\mathbf{p}_i$  is the corresponding momentum operator of the electron  $i$ ,  $\boldsymbol{\epsilon}_{q'\nu'k'_z}$  is the polarization vector of the photon, and  $H_{\nu'}^{(1)}(q'\rho)$  is the Hankel function.

The essential quantity involved is the matrix element of  $H'$  between the ground state  $|G\rangle$  and the exciton state  $|\nu, k_z\rangle$ . We know that the interaction matrix elements of  $H'$  can be written as

$$\langle \nu, k_z | H' | G \rangle = \sum_{l, \varphi} \langle c, (l, \varphi); \nu, (l, \varphi) | U_{\nu k_z}^*(l, \varphi) H' | G \rangle, \quad (4)$$

because the exciton state can be expressed as

$$|\nu, k_z\rangle = \sum_{l, \varphi} U_{\nu k_z}^*(l, \varphi) |c, (l, \varphi); \nu, (l, \varphi)\rangle, \quad (5)$$

in which the excited state  $|c, (l, \varphi); \nu, (l, \varphi)\rangle$  is defined as

$$|c, (l, \varphi); \nu, (l, \varphi)\rangle = a_{c, (l, \varphi)}^\dagger a_{\nu, (l, \varphi)} |G\rangle, \quad (6)$$

where  $a_{c, (l, \varphi)}^\dagger$  ( $a_{\nu, (l, \varphi)}$ ) is the creation (destruction) operator of an electron in the conduction (valence) band at lattice site  $(l, \varphi)$ . The expansion coefficient  $U_{\nu k_z}^*(l, \varphi)$  is the exciton wave function in the cylindrical tubule:

$$U_{\nu k_z}^*(l, \varphi) = \frac{1}{\sqrt{N}} \frac{1}{\sqrt{N'}} e^{i\nu\varphi + ik_z l}, \quad (7)$$

where the coefficient  $1/\sqrt{N'}$  is for the normalization of the state  $|\nu, k_z\rangle$ .

After summing over  $l$  and  $\varphi$  in Eq. (4), we have

$$\langle \nu, k_z | H' | G \rangle = \sum_{q' g n_\nu} \frac{e}{mc} \sqrt{\frac{2\pi\hbar c}{(q'^2 + (k_z + g)^2)^{1/2}v}} \times [b_{q', \nu+n_\nu, k_z+g} (\boldsymbol{\epsilon}_{q', \nu+n_\nu, k_z+g} \cdot \mathbf{A}_{\nu+n_\nu, k_z+g}) H_{\nu+n_\nu}^{(1)}(q'\rho) + \text{h.c.}], \quad (8)$$

where

$$\mathbf{A}_{\nu+n_\nu, k_z+g} = \sqrt{NN'} \int d^2\boldsymbol{\tau} \exp(i(k_z + g)\tau_z + i(\nu + n_\nu)\tau_\varphi) \times w_c(\boldsymbol{\tau}_z, \tau_\varphi) (-i\hbar\nabla) w_v(\boldsymbol{\tau}_z, \tau_\varphi), \quad (9)$$

,  $w_c(\boldsymbol{\tau}_z, \boldsymbol{\tau}_\varphi)$  and  $w_v(\boldsymbol{\tau}_z, \boldsymbol{\tau}_\varphi)$  are, respectively, the Wannier functions for the conduction band and the valence band at site 0, and  $g(n_\nu)$  is the reciprocal lattice in  $k_z$  ( $k_\varphi$ ) direction. Hence the interaction between the exciton and the photon (in the resonance approximation) can be written in the form

$$H' = \sum_{n_\nu, g} \sum_{q' \nu k_z} D_{q', \nu+n_\nu, k_z+g} b_{q', \nu+n_\nu, k_z+g} c_{\nu k_z}^\dagger + \text{h.c.}, \quad (10)$$

where

$$D_{q', \nu+n_\nu, k_z+g} = H_{\nu+n_\nu}^{(1)}(q' \rho) \boldsymbol{\epsilon}_{q', \nu+n_\nu, k_z+g} \cdot \mathbf{A}_{\nu+n_\nu, k_z+g} \times \frac{e}{mc} \sqrt{\frac{2\pi \hbar c}{(q'^2 + (k_z + g)^2)^{1/2} v}}. \quad (11)$$

Now, we assume that at time  $t = 0$  the exciton is in the mode  $\nu, k_z$ . For time  $t > 0$ , the state  $|\psi(t)\rangle$  can be written as

$$|\psi(t)\rangle = f_0(t) |\nu, k_z; 0\rangle + \sum_{q' n_\nu g} f_{G; q', \nu+n_\nu, k_z+g}(t) |G; q', \nu+n_\nu, k_z+g\rangle, \quad (12)$$

where  $|\nu, k_z; 0\rangle$  is the state with an exciton in the mode  $\nu, k_z$  in the cylindrical quantum wire,  $|G; q', \nu+n_\nu, k_z+g\rangle$  represents the state in which the electron-hole pair recombines and a photon in the mode  $q', \nu+n_\nu, k_z+g$  is created, and  $f_0(t)$  and  $f_{G; q', \nu+n_\nu, k_z+g}(t)$  are, respectively, the probability amplitudes of the state  $|\nu, k_z; 0\rangle$  and  $|G; q', \nu+n_\nu, k_z+g\rangle$ .

In the resonance approximation, the probability amplitude  $f_0(t)$  can be expressed as[7]

$$f_0(t) = \exp(-i\Omega_{\nu k_z} t - \frac{1}{2}\gamma_{\nu k_z} t), \quad (13)$$

where

$$\gamma_{\nu k_z} = 2\pi \sum_{q' n_\nu g} |D_{q', \nu+n_\nu, k_z+g}|^2 \delta(\omega_{q', \nu+n_\nu, k_z+g}) \quad (14)$$

and

$$\Omega_{\nu k_z} = \mathcal{P} \sum_{q' n_\nu g} \frac{|D_{q', \nu+n_\nu, k_z+g}|^2}{\omega_{q', \nu+n_\nu, k_z+g}} \quad (15)$$

with  $\omega_{q', \nu+n_\nu, k_z+g} = E_{\nu+n_\nu, k_z+g}/\hbar - c\sqrt{q'^2 + (k_z + g)^2}$ . Here  $\gamma_{\nu k_z}$  and  $\Omega_{\nu k_z}$  are, respectively, the decay rate and frequency shift of the exciton. And  $\mathcal{P}$  means the principal value of the integral.

If we neglect the Umklapp process, the exciton decay rate in the optical region can be calculated straightforwardly and is given by

$$\gamma_{\nu k_z} = \begin{cases} \frac{3}{2}\pi^2 \gamma_0 \frac{\rho}{d} \frac{1}{k_0 d} \left| H_\nu^{(1)}(\rho \sqrt{k_\nu^2 - k_z^2}) \right|^2, & k_z < k_\nu \\ 0, & \text{otherwise} \end{cases}, \quad (16)$$

where  $k_\nu = E_{k_z \nu}/\hbar = k_0 + \frac{\hbar^2 \nu^2}{2\mu \rho^2}$ ,

$$\gamma_0 = \frac{4e^2 \hbar k_0}{3m^2 c^2} |\boldsymbol{\chi}|^2, \quad (17)$$

and

$$\boldsymbol{\chi} = \int d^2 \boldsymbol{\tau} w_c(\boldsymbol{\tau}_z, \boldsymbol{\tau}_\varphi) (-i\hbar \boldsymbol{\nabla}) w_v(\boldsymbol{\tau}_z, \boldsymbol{\tau}_\varphi). \quad (18)$$

Here,  $\mu$  is the effective mass of the exciton,  $\boldsymbol{\chi}^*$  represents the single-atom dipole matrix element for an electron jumping from the excited state in the conduction band back to the hole state in the valence band, and  $\gamma_0$  is the decay rate of an isolated atom. We see from Eq. (16) that  $\gamma_{k_z \nu}$  is proportional to  $1/(k_0 d)$  and  $\rho/d$ . This is just the superradiance factor coming from the coherent contributions of atoms. If  $k_z$  is larger than  $k_\nu$ , these excitonic modes (trapped modes) are not capable of radiative decay. This is simply because the energy  $\hbar c k_\nu$  of that exciton is not sufficient to produce a photon.

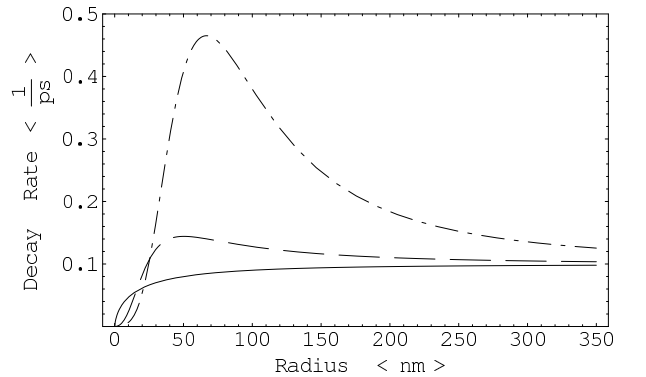


FIG. 2: Decay Rate of the superradiant exciton as a function of the wire radius. The vertical and horizontal units are  $\text{ps}^{-1}$  and  $\text{nm}$ , respectively. And the solid, dashed, and dot-dashed lines represent the  $\nu = 0, 1,$  and  $2$  modes, respectively. In this and following graph the parameters of a GaAs quantum well are chosen to obtain the numerical results.

In Fig. 2 we plot the decay rate  $\gamma_{\nu k_z}$  as a function of wire radius. Our numerical results are obtained by employing the data of GaAs (band gap is 1.52 eV). For  $\nu = 0$  mode (solid line), the decay rate increases with the increasing of wire radius and approaches 2D limit as  $\rho$  is large comparing to the wavelength of the emitted photon in a 2D thin film. For higher modes ( $\nu = 1, 2$ ), the results

depend on the kinetic energy  $\frac{\hbar^2 \nu^2}{2\mu\rho^2}$ . As can be seen from the figure, the decay rate also approaches 2D limit for large radius. On the other hand, the decay rate increases as the wire radius is decreased until the maximum decay rate is attained. After that a further reducing of the radius leads to a sharp decrease of the decay rate. This is similar to the transition from 2D to 3D: the higher wave number modes have larger maximum decay rate[12]. One also notes in small radius regime, the decay rate of the higher mode is smaller than that of the lower mode, i.e.  $\gamma_{\nu=2,k_z} > \gamma_{\nu=1,k_z} > \gamma_{\nu=0,k_z}$ . This phenomenon is also found in the quantum well system, and can be ascribed to the effects of interference[20]. Another interesting result is that the decay rate does not show any oscillatory dependence on radius while it shows oscillatory dependence on layer thickness in the case of the semiconductor thin film[11, 20]. The reason is that the angular momentum of the exciton is conserved in a cylindrical system, but, in a semiconductor thin film, the momentum is not conserved in the direction of broken symmetry. If we sum over all the sites in Eq. (4), the phase will run through a circle and thus preserve the same value.

One might suspect the practical value of our numerical results because our model is based on the one-layer assumption and the idealized assumptions, e.g. perfect cylindrical symmetry and infinite confinement. However, as we mentioned above, for the superradiant decay rate and frequency shift one only needs to replace the dipole matrix element with an effective one. This is why our result agrees well with that of a realistic GaAs quantum well in the large radius limit[10]. On the other hand, such an assumption may slightly deviate from the real case as the radius is small (e.g. as the radius approaches  $a_{ex}$ ). This is because the wavefunction of the exciton becomes more compact in the quantum wire with small radius limit, and it causes the increasing of the dipole matrix element  $\chi$  in Eq. (17). Besides, the quality of the quantum wire also influences the observation of the crossover, i.e. the thickness fluctuations should be controlled well, otherwise it will destroy the coherence in the circular direction.

Now let us turn to the results for the renormalized frequency shift. The frequency shift in Eq. (15) can be expressed as

$$\Omega_{\nu k_z} = \frac{\pi e^2 \hbar}{m^2 c^2 v} \mathcal{P} \sum_{q' n_\nu g} \frac{|\epsilon_{q', \nu+n_\nu, k_z+g} \cdot \mathbf{A}_{\nu+n_\nu, k_z+g}|^2}{\sqrt{q'^2 + (k_z + g)^2}} \times \frac{|H_{\nu+n_\nu}^{(1)}(q'\rho)|^2}{E_{\nu+n_\nu, k_z+g}/(\hbar c) - \sqrt{q'^2 + (k_z + g)^2}}. \quad (19)$$

As seen from above, the frequency shift suffers from ultraviolet divergence when  $g$  and  $n_\nu$  are large, and has infrared divergence when the denominator approaches zero. Following the procedure as shown in the work of Lee, Chuu, and Mei[19], the divergent problem is solved by renormalization.

In the usual renormalization procedure used in quantum field theory, the infinite quantities in Green function is subtracted by some infinite quantities to make them finite. The subtraction procedure is possible by substituting some finite physical quantities, such as renormalized masses, charges, and wave functions. The finite physical quantities observed from bare infinite quantities can be visualized, in the case of bare charge for example, as the polarization of vacuum. This is equivalent to say that there is virtual photon and opposite charged electron cloud surrounding the bare charge making the charge measured from outside become finite—a phenomena similar to that of shielding in dielectric material. But the renormalization procedure in quantum field theory is for free electrons. In the case of the condensed matter, the electrons are confined by periodic potential and complex interactions. Borrowing from the concepts of renormalization used in quantum field theory, we have

$$\Omega_{\nu k_z}^{ren} = \Omega_{\nu k_z} - \lim_{k_0 \rightarrow 0, d \rightarrow \infty} \Omega_{\nu k_z}, \quad (20)$$

where the two limiting processes  $k_0 \rightarrow 0$  and  $d \rightarrow \infty$  reduce the exciton to a free electron. In the limiting process  $d \rightarrow \infty$ , the ordinary exciton becomes a lone exciton standing alone in an empty lattice with no interaction with other atoms. And the process  $k_0 \rightarrow 0$  means that there is no energy difference between electron and hole.

We will now show that the ultraviolet divergence comes from the inclusion of Umklapp process. Define

$$\Omega_{\nu k_z}(l, \varphi) = \sum_{k_2 n_\varphi} J_{\nu k_z}(k_2, n_\varphi) \exp(ik_2 l + in_\varphi \varphi) \quad (21)$$

with

$$J_{\nu k_z}(k_2, n_\varphi) = \frac{\pi e^2 \hbar}{m^2 c^2 v} \mathcal{P} \sum_{q'} \frac{|\epsilon_{q' n_\varphi k_2} \cdot \chi|^2}{\sqrt{q'^2 + k_2^2}} \times \frac{|H_{n_\varphi}^{(1)}(q'\rho)|^2}{E_{n_\varphi k_2}/(\hbar c) - \sqrt{q'^2 + k_2^2}}. \quad (22)$$

From the above equations, we have

$$\begin{aligned} & \sum_{l, \varphi} \Omega_{\nu k_z}(l, \varphi) \exp(-ik_2 l - i\nu \varphi) \\ &= \sum_{k_2 n_\varphi} J_{\nu k_z}(k_2, n_\varphi) \sum_{l, \varphi} e^{i(k_2 - k_z)l + i(n_\varphi - \nu)\varphi} \\ &= N' N \sum_{g n_\nu} J_{\nu k_z}(k_z + g, \nu + n_\nu) \\ &= \Omega_{\nu k_z}. \end{aligned} \quad (23)$$

And from Eq. (21) we have  $\lim_{d \rightarrow 0} \Omega_{\nu k_z} = \Omega_{\nu k_z}(l = 0, \varphi = 0)$ , so we can rewrite the renormalized frequency

shift  $\Omega_{\nu k_z}^{ren}$  as

$$\Omega_{\nu k_z}^{ren} = \Omega_{\nu k_z}^{ren}(0, 0) + \Omega_{\nu k_z}^{coh} \quad (24)$$

with

$$\Omega_{\nu k_z}^{ren}(0, 0) = \Omega_{\nu k_z}(0, 0) - \lim_{k_0 \rightarrow 0} \Omega_{\nu k_z}(0, 0) \quad (25)$$

and

$$\Omega_{\nu k_z}^{coh} = \sum_{\substack{l \neq 0 \\ \varphi \neq 0}} e^{-i(k_z l + \nu \varphi)} \Omega_{\nu k_z}(l, \varphi). \quad (26)$$

As can be seen from Eq. (25), the renormalization affects only the part  $\Omega_{\nu k_z}(0, 0)$ —the frequency shift of the lone exciton in an empty lattice—and thus nothing to do with the correlation within the crystals. The coherent part  $\Omega_{\nu k_z}^{coh}$  in Eqs. (24) and (26) is not touched by renormalization procedure. The separation of  $\Omega_{\nu k_z}$  into two parts as shown in Eq. (24) is conceptually equivalent to singling out of the source term of quantum electrodynamical divergence in a correlated system.

Now we will investigate the origin of ultraviolet divergence. From Eq. (19) with the substitution  $\sum_{q'} \rightarrow \int \frac{q' dq'}{(2\pi/R^2)}$  and  $\sum_g \rightarrow \int \frac{dg}{(2\pi/L_z)}$ , we have

$$\begin{aligned} \Omega_{\nu k_z} &\simeq \frac{e^2 \hbar N'}{4\pi m^2 c^2} \mathcal{P} \sum_{n\nu} \int q' dq' \int dg \frac{|\boldsymbol{\epsilon}_{q', \nu+n\nu, k_z+g} \cdot \boldsymbol{\chi}|^2}{\sqrt{q'^2 + (k_z + g)^2}} \\ &\times \frac{|H_{\nu+n\nu}^{(1)}(q'\rho)|^2}{E_{\nu+n\nu, k_z+g}/(\hbar c) - \sqrt{q'^2 + (k_z + g)^2}}. \quad (27) \end{aligned}$$

It is noted that the result in Eq. (27) is the same as  $\Omega_{\nu k_z}(0, 0)$  from Eqs. (21) and (23). Hence we conclude that the ultraviolet divergence of  $\Omega_{\nu k_z}(0, 0)$  is really the same as that from Umklapp process of large  $g$  and  $n\nu$  that contribute to the full  $\Omega_{\nu k_z}$ . Once  $\Omega_{\nu k_z}(0, 0)$  of the lone exciton is rendered finite by renormalization via Eq. (25), the Umklapp processes of large  $g$  and  $n$  that arise from the unrestricted sum over  $l$  and  $\varphi$  will also be rendered finite simultaneously. Accordingly,  $\Omega_{\nu k_z}^{ren}$  can be written as

$$\Omega_{\nu k_z}^{ren} = \frac{\pi e^2 \hbar N'}{m^2 c^2 v} \mathcal{P} \sum_{q'} \frac{|\boldsymbol{\epsilon}_{q' \nu k_z} \cdot \boldsymbol{\chi}|^2}{\sqrt{q'^2 + k_z^2}} \frac{|H_{\nu}^{(1)}(q'\rho)|^2}{E_{\nu k_z}/(\hbar c) - \sqrt{q'^2 + k_z^2}}. \quad (28)$$

and thus the ultraviolet divergence problem is solved.

In the  $k_z \sim 0$  and  $\nu = 0$  mode, the renormalized result can be reduced as

$$\Omega_{\nu k_z}^{ren} = \frac{\pi e^2 \hbar N'}{m^2 c^2 v} \mathcal{P} \sum_{q'} \frac{|\boldsymbol{\epsilon}_{q' \nu k_z} \cdot \boldsymbol{\chi}|^2}{q'} \frac{|H_0^{(1)}(q'\rho)|^2}{k_0 - q'}. \quad (29)$$

As seen from above, the frequency shift suffers from infrared divergence when  $q' \sim 0$  or  $q' \sim k_0$ . This can be overcome by substituting  $-i\hbar\nabla$  by  $-imcq'\tau$  (Ref. 19) in Eq. (18) when  $q'$  is small. It is equivalent to the dipole interaction form,  $H' \sim \mathbf{r} \cdot \mathbf{E}$ . With this treatment, we have

$$\Omega_{\nu k_z}^{ren} \sim \frac{2\pi\rho}{d} N' \mathcal{P} \sum_{q'} \mathbf{B}_{q' \nu k_z} \frac{|H_0^{(1)}(q'\rho)|^2}{k_0 - q'} \quad (30)$$

with

$$\mathbf{B}_{q' \nu k_z} = \begin{cases} \frac{\pi e^2 \hbar}{m^2 c^2 v} |\boldsymbol{\epsilon}_{q' \nu k_z} \cdot \boldsymbol{\chi}|^2, & \text{when } q' \text{ is large} \\ \frac{\pi e^2 q'^2}{v} |\boldsymbol{\epsilon}_{q' \nu k_z} \cdot \mathbf{d}|^2, & \text{when } q' \text{ is small} \end{cases}, \quad (31)$$

where

$$\mathbf{d} = \int d^2 \boldsymbol{\tau} w_c(\boldsymbol{\tau}_z, \boldsymbol{\tau}_\varphi) \boldsymbol{\tau} w_v(\boldsymbol{\tau}_z, \boldsymbol{\tau}_\varphi). \quad (32)$$

Eq. (30) can not be evaluated analytically. But for large radius, the asymptotic form of Hankel function is :  $H_0^{(1)}(q'\rho) \sim \sqrt{2/(\pi q'\rho)} e^{iq'\rho}$ . And the renormalized frequency shift reduces to 2D limit[19]:

$$\Omega_{2D} = -\gamma_{\text{single}} \left(\frac{1}{k_0 d}\right)^2, \quad (33)$$

where

$$\gamma_{\text{single}} = \frac{2e^2}{\hbar c} \frac{E_{\nu, k_z \sim 0}}{\hbar} |k_0 \mathbf{d}|^2 \quad (34)$$

is the radiative decay rate of a single isolated exciton. Analogous to the decay rate, the renormalized frequency shift is explicitly seen to be coherently enhanced by the same factor  $(1/k_0 d)^2$  as a result of the interaction of the phase-matched photon amplitude with the delocalized excitonic amplitude in the plane. In Fig. 3, we numerically calculated the frequency shift as a function of wire radius. One can see from the figure the renormalized frequency shift does not show oscillatory dependence on radius, either. For  $\nu = 0$  mode, unlike the behavior of decay rate, the magnitude of the frequency shift first increases with the decreasing of radius. After reaching a minimum point, the frequency shift approaches to zero rapidly.

For usual semiconductors, the superradiant enhanced factor is about  $10^6$  for excitons in the optical range. However, due to the extreme smallness of  $\gamma_{\text{single}}$  itself, observation of  $\Omega_{\nu, k_z}$  is not expected to be easy. Its dependence on wire radius may be a useful feature to observe this quantity. Recently, R. A. Römer and M. E. Raikh studied theoretically the exciton absorption shredded by

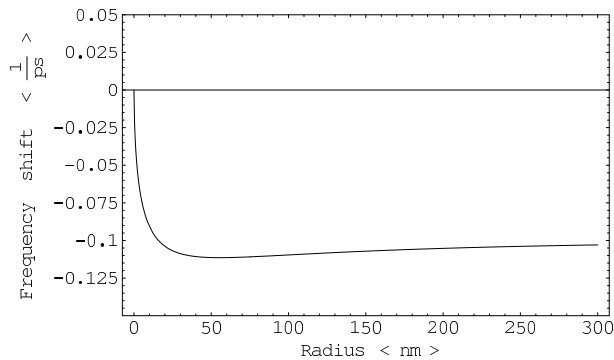


FIG. 3: Renormalized frequency shift of the superradiant exciton as a function of the wire radius. The vertical and horizontal units are  $\text{ps}^{-1}$  and  $\text{nm}$ , respectively.

a magnetic flux  $\Phi$  in a quantum ring[23]. They found the oscillator strength of the exciton is most enhanced when  $\Phi$  is equal to half of the universal flux quantum  $\Phi_0 = hc/e$ . And the oscillation period is equal to  $\Phi_0$ . Owing to the similarity in cylindrical geometry, the de-

cay rate and the frequency shift may be observed experimentally if one varies the magnetic flux or the wire radius.

In summary, we have calculated the decay rate of the superradiant exciton in a hollow cylindrical quantum wire. Similar to the case in a quantum well, the higher wave number modes are shown to have larger maximum decay rate. It is also found the decay rate does not show any oscillatory dependence on wire radius because of the conservation of the angular momentum in the cylindrical system. On the other hand, the frequency shift of the exciton is properly renormalized by removing the ultraviolet and infrared divergence. It is found the shift does not show oscillatory dependence on the radius, either. Some distinguishing features are pointed out and may be observed in a suitably designed experiment.

We would like to thank Professor M. F. Lin of National Cheng Kung University for a helpful discussion. This work is supported partially by the National Science Council, Taiwan under the grant number NSC 91-2112-M-009-012.

- 
- [1] R. H. Dicke, Phys. Rev. **93**, 99 (1954).
  - [2] N. Skribanowitz, I. P. Herman, J. C. MacGillivray, and M. S. Feld, Phys. Rev. Lett. **30**, 309 (1973).
  - [3] M. Gross, C. Fabre, P. Pillet, and S. Haroche, Phys. Rev. Lett. **36**, 1035 (1976).
  - [4] V. Ernst and P. Stehle, Phys. Rev. **176**, **1456** (1968).
  - [5] Y. C. Lee and D. L. Lin, Phys. Rev. **183**, 147 (1969); **183**, 150 (1969).
  - [6] J. J. Hopfield, Phys. Rev. **112**, 1555 (1958).
  - [7] K. C. Liu and Y. C. Lee, Physica **102A**, 131 (1980).
  - [8] U. Cebulla, G. Bacher, A. Forchel, G. Mayer, and W. T. Tsang, Phys. Rev. **B 39**, 6257 (1989).
  - [9] O. Brandt, G. C. La Rocca, A. Heberle, A. Ruiz, and K. Ploog, Phys. Rev. **B 45**, 3803 (1992).
  - [10] E. Hanamura, Phys. Rev. **B 38**, 1228 (1988).
  - [11] J. Knoester, Phys. Rev. Lett. **68**, 654 (1992).
  - [12] G. Björk, S. Pau, J. M. Jacobson, H. Cao, and Y. Yamamoto, Phys. Rev. **B 52**, 17310 (1995).
  - [13] V. M. Agranovich, D. M. Basko, and O. A. Dubovsky, J. Chem. Phys. **106**, 3896 (1997).
  - [14] V. Agranovich and O. Dubovsky, JETP Letters **3**, 223 (1966).
  - [15] Ya. Aaviksoo, Ya. Lippmaa, and T. Reinot, Optics and Spectroscopy (USSR) **62**, 419 (1987).
  - [16] A. L. Ivanov and H. Haug, Phys. Rev. Lett. **71**, 3182 (1993).
  - [17] Y. Manabe, T. Tokihiro, and E. Hanamura, Phys. Rev. **B 48**, 2773 (1993).
  - [18] Y. N. Chen and D. S. Chuu, T. Brandes, and B. Kramer, Phys. Rev. **B 64**, 125307 (2001).
  - [19] Y. C. Lee, D. S. Chuu, and W. N. Mei, Phys. Rev. Lett. **69**, 1081 (1992).
  - [20] Y. N. Chen and D. S. Chuu, Phys. Rev. **B 61**, 10815 (2000).
  - [21] K. Suenaga, C. Colliex, N. Demoncy, A. Loiseau, H. Pascard, and F. Willaime, Science **278**, 653 (1997).
  - [22] Y. Zhang, K. Suenaga, C. Colliex, and S. Iijima, Science **281**, 973 (1998).
  - [23] R. A. Römer and M. E. Raikh, Phys. Rev. **B 62**, 7045 (2000).